A Novel Statistical Process Control Approach for PM2.5 Monitoring Using Time Series Modeling

Yadpirun Supharakonsakun [1]* , Yupaporn Areepong [2]

[1] *Faculty of Science and Technology, Phetchabun Rajabhat University, Phetchabun 67000, Thailand.*

[2] *Faculty of Applied Science, King Mongkut's University of Technology Bangkok, Bangkok 10800, Thailand.*

Abstract

This research seeks to create a novel control chart capable of managing autocorrelated time series data by proposing a modified Exponentially Weighted Moving Average (EWMA) approach tailored to processes following the ARMA(p,q) model, which also makes use of exponential white noise. The key methodological contribution involves an explicit formula to compute the Average Run Length (ARL), while the Numerical Integral Equation (NIE) approach is utilized for verification purposes. The proposed formula not only demonstrated 100% agreement with NIE results but also significantly reduced computational time, requiring less than 0.001 seconds per run, compared to the 3–4 seconds typically needed by NIE. To assess the performance, simulation experiments and real-world case studies on PM2.5 air pollution data from Nakhon Phanom, Nan, and Nonthaburi provinces in Thailand were conducted. Our modified control chart was better at identifying minimal changes than a standard EWMA chart, as shown by lower ARL1, SDRL1, AEQL, and optimal PCI values. The one-sided chart structure, designed to monitor upward shifts in pollutant levels, further supports its application in environmental surveillance. Overall, the study introduces a fast, accurate, and practical tool for quality control in autocorrelated environments, offering both analytical and computational advantages over existing methods.

1- Introduction

Air serves as an essential element in the context of human survival, as it is required for respiration and facilitates the circulation of necessary minerals within the body. Similarly, other living organisms rely on air, with plants using it for photosynthesis. On a larger scale, air plays a crucial role in maintaining Earth's equilibrium, acting as a protective shield against harmful solar radiation, regulating global temperatures, enabling combustion, and serving as a medium for sound propagation.

However, the air we breathe today is heavily contaminated with fine dust particles and pollutants, posing significant health risks. Among these hazardous particulates, PM2.5 (for which the diameter does not exceed 2.5 microns) is especially dangerous. Since they are tiny, PM2.5 particles cannot be seen by the naked eye but can appear as haze or smoke when present at high concentrations. PM2.5 can be generated via road transport emissions, smoking tobacco products, the open burning of waste, agricultural residues, and industrial fuel combustion [1-3]. These fine particles often combine with other pollutants, such as hydrocarbons and heavy metals, making them even more harmful.

Because of their small size, PM2.5 particles can bypass the nasal filtration system, entering the respiratory tract before penetrating the alveoli. Subsequently, they proceed to the bloodstream, potentially causing severe complications. Even

---

when exposed to PM2.5 at high levels for only short periods of time, individuals can face increased risk of eye irritation, nasal inflammation, and throat pain. The respiratory system is particularly vulnerable, with symptoms including coughing and phlegm production. Individuals with preexisting health concerns, including allergies and diseases characterized by breathing problems, are more likely to experience worsening symptoms, while over the longer term, PM2.5 exposure is known to heighten the incidence of lung cancer and cardiovascular diseases [2, 4-5]. Recognizing its dangers, the WHO has classified PM2.5 as a Group 1 carcinogen [2]. Additionally, a report from the World Bank highlights that atmospheric contamination is a factor in the deaths of around 50,000 people each year in Thailand, imposing a significant economic burden on the country [6].

In recent years, Thailand has experienced recurring air pollution crises, with PM2.5 levels frequently exceeding safety thresholds [7, 8]. As a result, the country has consistently ranked among the worst in terms of air quality indices worldwide, according to the United States Air Quality Index (US AQI) [9]. The situation worsens during winter and early summer due to high atmospheric pressure, temperature inversion, and stagnant air, which prevent pollutants from dispersing. Wildfires and seasonal agricultural burning further exacerbate this problem. Metropolitan areas such as Bangkok and its surrounding provinces experience prolonged periods in which PM2.5 levels exceed safety standards. Moreover, northern provinces, particularly Chiang Mai and Phetchabun, face severe pollution due to forest fires along with the annual farming practice of setting fire to crop residues, most notably sugarcane, corn, and rice [6].

PM2.5 pollution poses significant environmental and public health challenges. Prolonged exposure can lead to respiratory and cardiovascular problems while also affecting visibility and limiting outdoor activities. Therefore, preventive measures and continuous monitoring are essential to mitigate these impacts. Accurate tracking of PM2.5 levels enables timely interventions and plays a critical role in formulating effective pollution control strategies [10, 11]. Where it is necessary to implement procedures for quality control and the tracking of specific processes, one common approach involves the use of Statistical Process Control (SPC), which maintains process stability and minimizes variability. According to Montgomery [12], SPC encompasses seven fundamental tools, with control charts being among the most prominent. In addition to their application in the manufacturing sector, control charts are also useful in environmental monitoring applications, such as measuring differences arising in temperature, air quality, or the presence of pollutants [13–15].

Since Shewhart [16] first proposed the use of control charts, several enhancements have been proposed. Among these, Page contributed the cumulative sum (CUSUM) chart [17] while Roberts [18] offered the exponentially weighted moving average (EWMA) chart. Both are able to detect even minor adjustments in processes. The popularity of EWMA charts, in particular, can be attributed to their sensitivity and robustness in nonnormal and autocorrelated data environments [12, 19, 20]. To address the limitations of the traditional EWMA chart, several researchers have proposed modifications. Patel & Divecha [21] developed a modified EWMA statistic which utilized the differences between successive observations, improving its responsiveness to small and sudden shifts. Later, Khan et al. [22] refined this approach by adding a constant term, enhancing its performance in autocorrelated data settings and nonnormal distributions [23–25]. These modified EWMA charts have since demonstrated strong practical utility across various real-world and industrial scenarios [26–28].

Despite these advancements, many existing studies assume normally distributed, independent observations, which is not always realistic for environmental or industrial data. In particular, air quality data such as PM2.5 often exhibit autocorrelation fluctuations. However, few studies have investigated how modified EWMA control charts perform under complex autocorrelated models such as Autoregressive Moving Average (ARMA) processes with nonnormal error distributions. To better reflect the real-world characteristics of PM2.5 data—which are nonnegative, right-skewed, and time-dependent—this study models the innovation process as exponentially distributed white noise rather than Gaussian noise. This assumption captures the asymmetric behavior of environmental fluctuations more effectively.

Our research examines the ARL performance of a modified EWMA chart under ARMA(p,q) procedures with exponentially distributed white noise in response to the observed gap in the literature. We propose an explicit ARL formula derived through the use of a second-type Fredholm integral equation and compare its results with those acquired via the NIE approach, aiming to assess the computational efficiency of these methods along with their accuracy. Our proposed control chart is then tested with real-world PM2.5 concentration data from three provinces in Thailand: Nakhon Phanom, Nan, and Nonthaburi.

This study also seeks to present information to guide the reader through both the theoretical development and practical application of our method. In Section 2, the fundamental attributes of the control charts encompassing both standard and modified EWMA are discussed, highlighting key differences and motivations for the modification. Section 3 provides a detailed derivation of the modified EWMA chart ARL, specifically under the ARMA(p,q) procedure with exponentially distributed white noise. In Section 4, a simulation is described, whereby authentic PM2.5 data are used in conjunction with our proposed control chart, demonstrating its practical effectiveness. In Section 5, the results are examined in the practical context in addition to consideration of the methodological contributions. To conclude, Section 6 then presents a summary of the principal findings, and suggests areas of interest for future studies.

2- Characteristics of Standard EWMA and Modified EWMA Control Charts

Characteristics of both standard and modified EWMA charts are described below. Although standard EWMA charts are relatively effective in identifying minor changes to process means, the modified version offers improved performance, particularly in handling autocorrelation and process-specific dynamics.

2-1- Standard EWMA Chart

The purpose of a standard EWMA chart is to detect minor process mean changes. It can be defined as:

$$E_t = (1-\lambda)Z_{t-1} + \lambda Y_t \ ; t = 1, 2, 3, \dots ,\tag{1}$$

in which E_t serves as the EWMA statistic, Y_t indicates the observation from the ARMA(p,q) procedure with exponential white noise, while the exponential smoothing parameter is given as $0 < \lambda \leq 1$.

If E_t violates the limit boundaries, a signal indicating an out-of-control scenario is generated. The stopping time τ_h represents the first point in time at which this occurs and has the definition:

$$\tau_h = \inf\{t > 0; E_t < g \text{ or } E_t > h\} ,\tag{2}$$

in which a represents the LCL while b represents the UCL.

The ARMA(p,q) procedure in the case of the standard EWMA control chart has an ARL for which the starting value $(E_0 = u)$ can be determined via $L(u)$:

$$L(u) = \text{ARL} = E_\infty(\tau_h) \geq T ,\tag{3}$$

in which T indicates a constant of sufficient size and where $E_\infty(.)$ denotes the expected value, assuming observations ε_t follow the distribution $F(y_t, \alpha)$.

Meanwhile, for the EWMA statistic:

$$E(E_t) = \mu ,\tag{4}$$

and

$$Var(E_t) = \left(\frac{\lambda}{2-\lambda}\right)\sigma^2 .\tag{5}$$

The boundaries denoted as UCL and LCL are determined as shown below for the EWMA control chart:

$$\text{UCL, LCL} = \mu_0 \pm K_1\sigma\sqrt{\frac{\lambda}{(2-\lambda)}} ,\tag{6}$$

where μ_0 is the target mean, σ is the standard deviation of E_t, and K_1 is a control limit multiplier.

2-2- Modified EWMA Control Chart

An enhanced EWMA chart was described by Khan et al. [22] which builds upon the modified statistic initially introduced by Patel & Divecha [21]. This chart integrates both past and present process information and can be explained as follows:

$$M_t = (1-\lambda)M_{t-1} + \lambda Y_t + k(Y_t - Y_{t-1}) \ ; t = 1, 2, 3, \dots ,\tag{7}$$

in which M_t represents the modified EWMA statistic for the ARMA(p,q) procedure with exponential white noise, $\lambda \in (0,1]$ represents an exponential smoothing parameter, and the constant, k, is non-negative.

The stopping time τ_b is defined as the first time point when M_t has a value which falls outside the boundaries defined by the UCL value or the LCL value:

$$\tau_b = \inf\{t \geq 1; M_t \notin (a, b)\} .\tag{8}$$

The ARMA(p,q) process using this chart with an initial value has an ARL which is evaluated via the function $G(u)$:

$$G(u) = E_\infty[\tau_b | M_0 = u] .\tag{9}$$

The modified EWMA chart has a mean and variance given as:

$$E(M_t) = \mu, \tag{10}$$

and

$$Var(M_t) = \frac{(\lambda + 2\lambda k + 2k^2)\sigma^2}{(2-\lambda)}. \tag{11}$$

The modified EWMA chart has control limits (CLs) which are determined as:

$$\text{UCL, LCL} = \mu_0 \pm K_2 \sigma \sqrt{\frac{(\lambda + 2\lambda k + 2k^2)}{(2-\lambda)}}, \tag{12}$$

where K_2 is the control limit multiplier for the modified chart.

3- ARL Derivation for ARMA(p,q) Procedure on the Modified EWMA Chart

Applications involving seasonal or periodic data, such as climate and economic time series are well-suited to the ARMA(p,q) procedure. It is defined as follows:

$$X_t = \mu + \varepsilon_t + \phi_1 X_{t-1} + \phi_2 X_{t-2} + \ldots + \phi_p X_{t-p} - \theta_1 \varepsilon_{t-1} - \theta_2 \varepsilon_{t-2} - \ldots - \theta_q \varepsilon_{t-q} \quad ; t = 1, 2, 3, \ldots, \tag{13}$$

in which μ is constant, $\phi_i ; i = 1, 2, 3, \ldots, p$ is an autoregressive coefficient, $\theta_i ; i = 1, 2, 3, \ldots, q$ is the coefficient of the moving average, while $\varepsilon_t \sim Exp(\alpha)$ is an i.i.d. white noise error term assumed to follow an exponential distribution

3-1- Explicit ARL Formula

The analytical expression for the modified EWMA chart ARL via ARMA(p,q) is derived as described below:

Phase 1: Substitute X_t into the modified EWMA statistic

The process begins by inserting the expression for X_t from Equation 13 into M_t, as defined in Equation 7. This results in a reformulated version of the modified EWMA statistic:

$$M_t = (1-\lambda)Z_{t-1} + (\lambda + k)\varepsilon_t + (\lambda + k)\mu + (\lambda\phi_1 + k\phi_1 - k)X_{t-1} + (\lambda\phi_2 + k\phi_2)X_{t-2} + \ldots + (\lambda\phi_p + k\phi_p)X_{t-p} - (\lambda\theta_1 + k\theta_1)\varepsilon_{t-1} - (\lambda\theta_2 + k\theta_2)\varepsilon_{t-2} - \ldots - (\lambda\theta_q + k\theta_q)\varepsilon_{t-q}. \tag{14}$$

Phase 2: Defining Initial Time and Rewriting Expressions

The analysis begins at time $t = 1$, assigning $M_0 = u, X_0 = \varsigma$ and $\varepsilon_0 = \gamma$. Therefore, the equation can be expressed as:

$$M_1 = (1-\lambda)u + (\lambda + k)\varepsilon_1 + (\lambda + k)\mu + (\lambda\phi_1 + k\phi_1 - k)\varsigma - (\lambda + k)\theta_1\gamma + (\lambda + k)\phi_2 X_{t-2} + \ldots + (\lambda + k)\phi_p X_{t-p} - (\lambda + k)\theta_2\varepsilon_{t-2} - \ldots - (\lambda + k)\theta_q\varepsilon_{t-q}. \tag{15}$$

Phase 3: Establishing Control Limits for the In-Control Case

Here, ε_1 represents the random variable for an in-control process. M_1 has a control region defined as $0 < M_1 < b$, corresponding to the LCL and UCL. This boundary condition is restated on the formulation in Section 2.2.

$$0 < (1-\lambda)u + (\lambda + k)\varepsilon_1 + (\lambda + k)\mu + (\lambda\phi_1 + k\phi_1 - k)\varsigma - (\lambda + k)\theta_1\gamma + (\lambda + k)\phi_2 X_{t-2} + \ldots + (\lambda + k)\phi_p X_{t-p} - (\lambda + k)\theta_2\varepsilon_{t-2} - \ldots - (\lambda + k)\theta_q\varepsilon_{t-q} < b \tag{16}$$

Phase 4: Reformulating in Terms of ε_1

To simplify, the expressions in terms of A and B are introduced:

$$A = (\lambda\phi_1 + k\phi_1 - k)\varsigma \text{ and } B = (\lambda + k)\phi_2 X_{t-2} + \ldots + (\lambda + k)\phi_p X_{t-p} - (\lambda + k)\theta_1\gamma - (\lambda + k)\theta_2\varepsilon_{t-2} - \ldots - (\lambda + k)\theta_q\varepsilon_{t-q}.$$

These allow ε_1 to be expressed in a more concise form for substitution into later calculations.

$$\frac{-(1-\lambda)u - (\lambda + k)\mu - A}{\lambda + k} - B < \varepsilon_1 < \frac{b - (1-\lambda)u - (\lambda + k)\mu - A}{\lambda + k} - B \tag{17}$$

Phase 5: Application of the Fredholm Integral Equation

The analytical expression representing the ARL is obtained via the Fredholm integral equation of the second kind. Let $Q(u)$ serve as the function representing the explicit ARL for the modified EWMA chart on the ARMA(p,q) process, expressed as shown:

$$(u) = 1 + \frac{1}{\lambda+k} \int_{\frac{-(1-\lambda)u-(\lambda+k)\mu-A}{\lambda+k}-B}^{\frac{b-(1-\lambda)u-(\lambda+k)\mu-A}{\lambda+k}-B} Q(M_1) f(\varepsilon_1) d\varepsilon_1. \tag{18}$$

Define $\psi = M_1$. Thus, $\frac{d\psi}{d\varepsilon_1} = \lambda + k$. This transformation leads to a modified integral formulation as follows:

$$Q(u) = 1 + \frac{1}{\lambda+k} \int_0^b Q(\psi) f\left(\frac{\psi-(1-\lambda)u-(\lambda+k)\mu-A}{\lambda+k} - B\right) d\psi. \tag{19}$$

Phase 6: Verifying the Solution Explicit ARL

Equation 19 is used to verify that the derived ARL satisfies the required existence and uniqueness conditions based on the fixed-point theorem introduced in Section 3.3. Assuming that $\varepsilon_1 \sim Exp(\alpha)$, further developments are made as follows:

$$Q(u) = 1 + \frac{1}{\lambda+k} \int_0^b Q(\psi) \frac{1}{\alpha} e^{-\left(\frac{\psi-(1-\lambda)u-(\lambda+k)\mu-A}{(\lambda+k)\alpha} - \frac{B}{\alpha}\right)} d\psi = 1 + \frac{1}{(\lambda+k)\alpha} e^{\frac{\psi-(1-\lambda)u-(\lambda+k)\mu-A}{(\lambda+k)\alpha} + \frac{B}{\alpha}} \int_0^b Q(\psi) e^{-\frac{\psi}{(\lambda+k)\alpha}} d\psi.$$

As previously stated, the variable ω is defined as $\int_0^b Q(\psi) e^{-\frac{\psi}{(\lambda+k)\alpha}} d\psi$, while $\rho(\psi)$ is assigned a value of $e^{\frac{\psi-(1-\lambda)u-(\lambda+k)\mu-A}{(\lambda+k)\alpha} + \frac{B}{\alpha}}$, leading to the following expression:

$$Q(u) = 1 + \frac{\omega \cdot \rho(\psi)}{(\lambda+k)\alpha}. \tag{20}$$

Following this, attention is directed to the variable ω.

$$\omega = \int_0^b Q(u) e^{-\frac{\psi}{(\lambda+k)\alpha}} d\psi = \int_0^b \left[1 + \frac{\omega \cdot \rho(\psi)}{(\lambda+k)\alpha}\right] e^{-\frac{\psi}{(\lambda+k)\alpha}} d\psi = \int_0^b e^{-\frac{\psi}{(\lambda+k)\alpha}} d\psi + \omega \int_0^b \frac{\rho(\psi)}{(\lambda+k)\alpha} e^{-\frac{\psi}{(\lambda+k)\alpha}} d\psi = -(\lambda+k)\alpha \left[e^{-\frac{b}{(\lambda+k)\alpha}} - 1\right] - \frac{\omega}{\lambda} e^{\frac{(\lambda+k)\mu+A}{(\lambda+k)\alpha} + \frac{B}{\alpha}} \left[e^{\frac{-\lambda b}{(\lambda+k)\alpha}} - 1\right]$$

The integral equation corresponding to ω is subsequently presented as follows:

$$\omega = \frac{-(\lambda+k)\alpha \left[e^{-\frac{b}{(\lambda+k)\alpha}} - 1\right]}{1 + \frac{1}{\lambda} e^{\frac{(\lambda+k)\mu+A+B}{(\lambda+k)\alpha}} \left[e^{\frac{-\lambda b}{(\lambda+k)\alpha}} - 1\right]} \tag{21}$$

To conclude, by inserting Equation 21 into Equation 20, the resulting expression for $Q(u)$ is obtained as follows

$$Q(u) = 1 + \frac{-(\lambda+k)\alpha \left[e^{-\frac{b}{(\lambda+k)\alpha}} - 1\right] - \frac{u}{\lambda} e^{\frac{A-B}{(\lambda+k)\alpha}} \left[e^{\frac{-\lambda b}{(\lambda+k)\alpha}} - 1\right] \cdot e^{\frac{u-A}{(\lambda+k)\alpha} + \frac{B}{\alpha}}}{(\lambda+k)\alpha} \cdot \left[\frac{-\beta(\lambda+k)\left[e^{-\frac{b}{(\lambda+k)\alpha}} - 1\right]}{1 + \frac{1}{\lambda} e^{A+B} \cdot e^{\frac{\mu}{\alpha}}\left[e^{-\frac{\lambda b}{(\lambda+k)\alpha}} - 1\right]}\right].$$

Ultimately, a simplified expression for $Q(u)$ is obtained as follows:

$$Q(u) = 1 - \frac{\lambda e^{\frac{(1-\lambda)u}{(\lambda+k)\alpha}} \left[e^{-\frac{b}{(\lambda+k)\alpha}} - 1\right]}{\lambda e^{-\frac{\mu}{\alpha}} \cdot e^{-\frac{A+B}{(\lambda+k)\alpha}} \left[e^{\frac{-\lambda b}{(\lambda+k)\alpha}} - 1\right]}. \tag{22}$$

Finally, by substituting A and B into Equation 22, the explicit formula giving the ARMA(p,q) procedure ARL with exponential white noise under the modified EWMA chart is obtained for both in-control ($\alpha = \alpha_0$) and out-of-control ($\alpha = \alpha_1; \alpha_1 = \alpha_0(1 + \delta)$) processes as follows:

$$ARL_0 = 1 - \frac{\lambda e^{\frac{(1-\lambda)u}{(\lambda+k)\alpha_0}} \left[e^{-\frac{b}{(\lambda+k)\alpha_0}} - 1\right]}{\lambda e^{\frac{-u}{\alpha_0}} \cdot e^{\frac{-(\lambda\phi_1+k\phi_1-k)\varsigma}{(\lambda+k)\alpha_0}} \cdot e^{-\frac{\theta_1\gamma+\phi_2 X_{t-2}+\dots+\phi_p X_{t-p}-\theta_2\varepsilon_{t-2}-\dots-\theta_q\varepsilon_{t-q}}{\alpha_0}} \left[e^{\frac{-\lambda b}{(\lambda+k)\alpha_0}} - 1\right]}, \tag{23}$$

and;

$$ARL_1 = 1 - \frac{\lambda e^{\frac{(1-\lambda)u}{(\lambda+k)\alpha_1}} \left[e^{-\frac{b}{(\lambda+k)\alpha_1}} - 1\right]}{\lambda e^{\frac{-u}{\alpha_1}} \cdot e^{\frac{-(\lambda\phi_1+k\phi_1-k)\varsigma}{(\lambda+k)\alpha_1}} \cdot e^{-\frac{\theta_1\gamma+\phi_2 X_{t-2}+\dots+\phi_p X_{t-p}-\theta_2\varepsilon_{t-2}-\dots-\theta_q\varepsilon_{t-q}}{\alpha_1}} \left[e^{\frac{-\lambda b}{(\lambda+k)\alpha_1}} - 1\right]}. \tag{24}$$

3-2- Numerical Integral Equation (NIE) Method for ARL Estimation

The NIE method, combined with quadrature rules, offers a precise and computationally efficient technique to estimate the ARL [29]. The ARMA(p,q) model with exponential white noise can be employed to analytically compute the ARL via the NIE approach in the case of the modified EWMA chart. The steps to follow for this computation are outlined below:

Phase 1: Applying the Gauss–Legendre quadrature rule

Let $\Upsilon(u)$ denote the modified EWMA chart ARL under the ARMA(p,q) model, estimated via the Gauss–Legendre rule. The solutions to n linear systems of equations can be used to evaluate the integral over the interval [0, b]. The quadrature rule provides an approximation of the integral as:

$$\int_0^b L(\varphi)f(\varphi)d\varphi \approx \sum_{j=1}^m w_j f(\varpi_j),\tag{25}$$

where $\varpi_j = \frac{b}{m}\left(j - \frac{1}{2}\right)$ for $j = 1,2,\dots,m$ while $w_j = \frac{b}{m}$ is the associated weight.

Phase 2: Expressing the ARL via the quadrature rule

The ARL function $\Upsilon(\varpi_i)$ can be calculated by:

$$\Upsilon(\varpi_i) = 1 + \frac{1}{\lambda+k}\sum_{j=1}^m w_j \Upsilon(\varpi_j)f\left(\frac{\varpi_j-(1-\lambda)u-(\lambda+k)\mu-A}{\lambda+k} - B\right), i = 1,2,\dots,m.\tag{26}$$

This system of equations can be rewritten for each ϖ_i, generating a system of n linear equations which appear concisely below:

$$M_{m\times1} = (I_m - R_{m\times m})^{-1}1_{m\times1}.\tag{27}$$

where $M_{m\times1} = [\Upsilon(\varpi_1), \Upsilon(\varpi_2),\dots,\Upsilon(\varpi_n)]^T$, $1_{m\times1}$ is a column vector of ones, and I_m is the identity matrix.

Phase 3: Constructing the Matrix $R_{m\times m}$

Therefore, matrix $R_{m\times m}$ consists of elements defined as:

$$R_{ij} \approx \frac{1}{\lambda+k}\sum_{j=1}^m w_j f\left(\frac{\varpi_j-(1-\lambda)u-(\lambda+k)\mu-A}{\lambda+k} - B\right).\tag{28}$$

If the matrix $(I - R)^{-1}$ exists, the solution for M is given by:

$$M_{m\times1} = (I_m - R_{m\times m})^{-1}1_{m\times1}.$$

Phase 4: Final Substitution and Expression

The substitution of ϖ_i using u in $\Upsilon(\varpi_i)$ enables the ARL to be expressed as:

$$\Upsilon(u) = 1 + \frac{1}{\lambda+k}\sum_{j=1}^m w_j \Upsilon(\varpi_j)f\left(\frac{\varpi_j-(1-\lambda)u-(\lambda+k)\mu-A}{\lambda+k} - B\right).\tag{29}$$

Thus, Equation 29 provides an approximation in numerical form for the integral equation for $\Upsilon(u)$, representing the ARL computed via the NIE method.

3-3- ARL Existence and Uniqueness

The fixed-point theorem of Banach may be employed in in the context of the ARL equation to establish the theoretical foundation for its existence and uniqueness [30]. This theorem ensures that the integral equation defining the explicit formulation of the ARL has a unique solution.

Consider T to serve as an operator acting upon a space of continuous functions, defined by the following integral transformation:

$$T\big(Q(u)\big) = 1 + \frac{1}{\lambda+k}\int_0^b Q(\psi) f\left(\frac{\psi-(1-\lambda)u-(\lambda+k)\mu-A}{\lambda+k} - B\right) d\psi.\tag{30}$$

If T indicates a contraction mapping, a unique solution $Q(u)$ exists such that $T\big(Q(u)\big) = Q(u)$, guaranteed by the aforementioned theorem associated with Banach.

This confirms that for Equation 30, a unique solution exists Equation 30.

Theorem 1: Banach's Fixed-Point Theorem

Let $T: X \rightarrow X$ represent a contraction mapping on a metric space (X, d) which has the contraction constant $0 < r \leq 1$. Subsequently, in the case of all $Q_1(u), Q_2(u) \in X$, it holds that $\left\|T(Q_1(u)) - T(Q_2(u))\right\| \leq r\|Q_1(u) - Q_2(u)\|$. This implies that there is a unique fixed point $Q(u) \in X$ for T whereby: $T(Q(u)) = Q(u)$.

Proof. It is necessary to establish whether T, as described in Equation 28, can be considered a contraction mapping. To do this, it is important to consider the set of functions $Q(u)$ on the interval $[0, b]$ under the supremum norm: $\|Q(u)\|_\infty = \sup\limits_{u \in [0,b]} |Q(u)|$.

We aim to show that for any $Q_1(u), Q_2(u) \in [0, b]$:

$$\left\|T(Q_1(u)) - T(Q_2(u))\right\|_\infty = \sup\limits_{u \in [0,b]} |Q_1(u) - Q_2(u)|$$

$$= \sup\limits_{u \in [0,b]} \left| \frac{\rho(u)}{(\lambda+k)\alpha} \int_0^b (Q_1(u) - Q_2(u)) e^{-\frac{\psi}{(\lambda+k)\alpha}} d\psi \right|$$

$$= \left\|T(Q_1(u)) - T(Q_2(u))\right\|_\infty \sup\limits_{u \in [0,b]} \left| \rho(u)\left(e^{\frac{-b}{(\lambda+k)\alpha}} - 1\right) \right|$$

$$\leq \sup\limits_{u \in [0,b]} \left| \left\|T(Q_1(u)) - T(Q_2(u))\right\|_\infty \rho(u)\left(e^{\frac{-b}{(\lambda+k)\alpha}} - 1\right) \right|$$

$$\leq r\left\|T(Q_1(u)) - T(Q_2(u))\right\|_\infty$$

where $r = \sup\limits_{u \in [0,b]} \left| \rho(u)\left(e^{\frac{-b}{(\lambda+k)\alpha}} - 1\right) \right|; 0 \leq r < 1.$

Hence, T satisfies the conditions of Banach's theorem, proving that Equation 30 presents a unique ARL solution, as indicated by the resulting unique fixed point.

4- Results

4-1- Simulation Outcomes

Comparisons are drawn to investigate the effectiveness of the NIE approach relative to the performance for the explicit formula for ARMA(p,q) models—specifically, ARMA(2,1), (1,2), (2,2), and (3,2)—through simulations using the modified EWMA chart. The comparisons are made through a sequence of steps presented as follows:

Phase 1: Calculate the necessary control limits associated with the ARMA(p,q) model before establishing the in-control ARL.

Then the in-control ARL_0 must be set as 370. Specification of the exponential white noise parameter (α_0) follows, along with the smoothing parameters, with the shift parameter δ set to 0. Using Equation 16, the UCL is calculated to achieve the desired ARL_0.

Phase 2: Calculate ARL_1 for the process which is out of control.

In the case of our out-of-control scenario, various shift values are considered: δ = 0.001, 0.003, 0.005, 0.007, 0.01, 0.03, 0.05, 0.07, 0.1, 0.5, 0.7 and 1. Using these values, ARL_1 is computed by applying the adjusted white noise parameter $\alpha_1 = \alpha_0(1 + \delta)$ (as defined in Equation 24), along with the UCL determined in Phase 1.

Phase 3: Estimate ARL_1 via the NIE approach.

The NIE approximation is implemented with 500 division points (m = 500). The simulations are executed via MATHEMATICA. In the case of the explicit formula ($CPU_{Q(u)}$) and NIE ($CPU_{\Upsilon(u)}$), computational times are recorded in seconds.

Phase 4: Compare the outcomes obtained via the explicit formula and NIE.

For accuracy assessment, ARL values derived via the explicit formula (denoted as $Q(u)$ in Equations 24 and 25) are compared with those from NIE (indicated as $\Upsilon(u)$ in Equation 28). The accuracy percentage (%Acc) can be calculated by:

$$\%\text{Acc} = \left(1 - \left|\frac{Q(u) - \Upsilon(u)}{Q(u)}\right|\right) \times 100. \tag{31}$$

Phanyaem [31] reports that this measure is equivalent to the absolute percentage difference (%Diff), serving as an effective indicator of approximation accuracy and calculated in the same manner as Equation 31.

Tables 1 and 2 present ARL findings acquired from the explicit formula and NIE. The model coefficients were varied, and the constant k was set to 0.5 for the modified EWMA chart, with the in-control ARL_0 fixed as 370. Procedures for computing the ARL values are illustrated in Figure 1.

Table 1. ARLs for ARMA(p,q) models on modified EWMA through an explicit formula and NIE for $\mu = 2, k = 0.5,$ $\lambda = 0.1$, ARL$_0$=370

Model	b	δ	$Q(u)$	CPU$_{Q(u)}$	$\Upsilon(u)$	CPU$\Upsilon(u)$	%Acc
ARMA(2,1) $\phi_i = 0.1, \theta_1 = 0.3$	0.20792	0.00	370.106538	<0.001	370.106522	3.672	100
		0.001	308.582474	<0.001	308.582463	3.953	100
		0.003	231.403436	<0.001	231.403429	3.719	100
		0.005	184.951290	<0.001	184.951284	3.766	100
		0.007	153.924375	<0.001	153.924371	3.656	100
		0.01	122.852656	<0.001	122.852653	3.672	100
		0.03	51.708738	<0.001	51.708737	3.922	100
		0.05	32.327947	<0.001	32.327946	3.734	100
		0.07	23.322060	<0.001	23.322060	3.656	100
		0.10	16.297411	<0.001	16.297411	3.672	100
		0.30	5.187343	<0.001	5.187343	3.843	100
		0.50	3.134262	<0.001	3.134262	3.656	100
		0.70	2.341598	<0.001	2.341598	3.578	100
		1.00	1.811784	<0.001	1.811784	3.625	100
ARMA(2,2) $\phi_i = 0.2, \theta_i = 0.4$	0.282549	0.00	370.115784	<0.001	370.115756	3.609	100
		0.001	314.031007	<0.001	314.030986	3.938	100
		0.003	240.832437	<0.001	240.832422	3.734	100
		0.005	195.167259	<0.001	195.167248	3.828	100
		0.007	163.961298	<0.001	163.961290	3.782	100
		0.01	132.125870	<0.001	132.125863	3.844	100
		0.03	56.934206	<0.001	56.934204	3.797	100
		0.05	35.868056	<0.001	35.868055	3.797	100
		0.07	25.986674	<0.001	25.986673	3.781	100
		0.10	18.233380	<0.001	18.233380	3.766	100
		0.30	5.848432	<0.001	5.848432	3.687	100
		0.50	3.518940	<0.001	3.518940	3.765	100
		0.70	2.607210	<0.001	2.607210	3.797	100
		1.00	1.989415	<0.001	1.989415	3.781	100
ARMA(3,3) $\phi_i = \theta_i = 0.3$	0.187792	0.00	370.011171	<0.001	370.011159	3.531	100
		0.001	306.740059	<0.001	306.740050	3.656	100
		0.003	228.378816	<0.001	228.378810	3.891	100
		0.005	181.747576	<0.001	181.747572	3.891	100
		0.007	150.820852	<0.001	150.820848	3.906	100
		0.01	120.024263	<0.001	120.024260	3.719	100
		0.03	50.163081	<0.001	50.163081	3.859	100
		0.05	31.289637	<0.001	31.289637	3.719	100
		0.07	22.543743	<0.001	22.543743	3.829	100
		0.10	15.733904	<0.001	15.733904	3.922	100
		0.30	4.996705	<0.001	4.996705	3.671	100
		0.50	3.023984	<0.001	3.023984	3.625	100
		0.70	2.265833	<0.001	2.265833	3.813	100
		1.00	1.761432	<0.001	1.761432	3.922	100

Table 2. ARLs for the ARMA(p,q) model on the modified EWMA through an explicit formula and NIE for $\mu = 2$, $k = 0.5, \lambda = 0.2$, **ARL₀=370**

| Model	b	δ	$Q(u)$	$\text{CPU}_{Q(u)}$	$\Upsilon(u)$	$\text{CPU}\Upsilon(u)$	%Acc
ARMA(1,2) $\phi_1 = -0.1, \theta_i = -0.3$	0.11843	0.00	370.216251	<0.001	370.216240	3.610	100
		0.001	273.912278	<0.001	273.912272	3.688	100
		0.003	180.050158	<0.001	180.050155	3.531	100
		0.005	134.007845	<0.001	134.007843	3.641	100
		0.007	106.661845	<0.001	106.661844	3.704	100
		0.01	81.604652	<0.001	81.604651	3.797	100
		0.03	31.547928	<0.001	31.547928	3.781	100
		0.05	19.414936	<0.001	19.414936	3.734	100
		0.07	13.969618	<0.001	13.969618	3.813	100
		0.10	9.803479	<0.001	9.803479	3.844	100
		0.30	3.356764	<0.001	3.356764	3.844	100
		0.50	2.186755	<0.001	2.186755	3.844	100
		0.70	1.738471	<0.001	1.738471	3.828	100
		1.00	1.441138	<0.001	1.441138	3.703	100
ARMA(2,2) $\phi_i = -0.5, \theta_i = -0.6$	0.160858	0.00	370.104580	<0.001	370.104560	3.672	100
		0.001	280.382680	<0.001	280.382668	3.829	100
		0.003	188.717042	<0.001	188.717036	3.875	100
		0.005	142.137182	<0.001	142.137178	3.703	100
		0.007	113.946827	<0.001	113.946824	3.735	100
		0.01	87.763359	<0.001	87.763357	3.672	100
		0.03	34.416037	<0.001	34.416037	3.890	100
		0.05	21.267783	<0.001	21.267782	3.968	100
		0.07	15.336043	<0.001	15.336043	3.719	100
		0.10	10.782264	<0.001	10.782264	3.859	100
		0.30	3.687386	<0.001	3.687386	3.719	100
		0.50	2.379891	<0.001	2.379891	3.672	100
		0.70	1.872199	<0.001	1.872199	3.750	100
		1.00	1.530721	<0.001	1.530721	3.688	100
ARMA(3,3) $\phi_i = -0.7, \theta_i = -0.8$	0.145218	0.00	370.019937	<0.001	370.019921	3.843	100
		0.001	278.133432	<0.001	278.133423	3.640	100
		0.003	185.719863	<0.001	185.719858	3.906	100
		0.005	139.315779	<0.001	139.315776	3.921	100
		0.007	111.411215	<0.001	111.411213	3.719	100
		0.01	85.613405	<0.001	85.613403	3.718	100
		0.03	33.407998	<0.001	33.407998	3.937	100
		0.05	20.615283	<0.001	20.615283	3.859	100
		0.07	14.854324	<0.001	14.854324	3.532	100
		0.10	10.436834	<0.001	10.436834	3.906	100
		0.30	3.570207	<0.001	3.570207	3.875	100
		0.50	2.311211	<0.001	2.311211	3.922	100
		0.70	1.824505	<0.001	1.824505	3.750	100
		1.00	1.498653	<0.001	1.498653	3.953	100
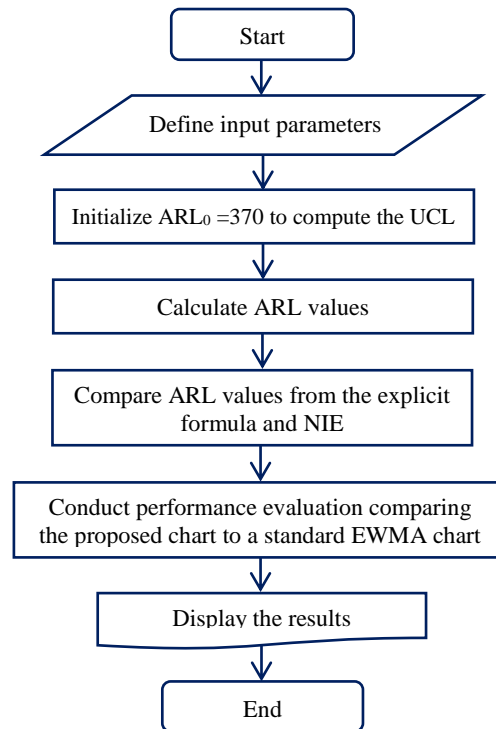
Figure 1. Flowchart of the study process

For Table 1, the models evaluated were ARMA(2,1), AR(2,2), and AR(3,3), whereas Table 2 includes ARMA(1,2), AR(2,2), and AR(3,3). These ARL values were calculated via both methods for smoothing parameters $\lambda = 0.1$ and 0.2. The results from the explicit formula and NIE approach appeared equivalent, and their agreement was assessed in terms of percentage accuracy (%Acc), which was 100% in all the cases. This perfect agreement confirms the mathematical soundness and reliability of the proposed explicit formula in replicating the standard NIE-based computation.

Despite the accuracy being identical, the explicit formula demonstrated a significant advantage in computation speed, requiring less than 0.001 seconds, compared with approximately 3–4 seconds for the NIE method. Therefore, the explicit formula proves to be a more efficient approach for estimating ARLs and is preferable for future comparisons of control chart performance. This improvement in computational time is especially crucial when applied to real-time monitoring systems, where immediate responsiveness is essential.

The next step involves drawing efficiency comparisons between the modified EWMA chart using the ARMA(p,q) procedure for ARL calculation under the explicit formula, and the original EWMA and EEWMA control charts. To do so, a range of scenarios are investigated to assess the relative performance. In addition to the ARL, other measures, including the SDRL (standard deviation of the run length), may be used to examine the abilities of different charts to detect conditions which are out of control [32].

For in-control processes, SDRL determination is performed using the following formulas:

$$ARL_0 = \frac{1}{\beta_0}, SDRL_0 = \sqrt{\frac{1-\beta_0}{\beta_0^2}}, \tag{32}$$

where β_0 represents the probability of obtaining an error of Type I. In this current research, ARL_0 is set to 370, while the corresponding $SDRL_0$ is approximated via Equation 32, which yields a similar value.

In the case of out-of-control processes, the SDRL can be calculated as:

$$ARL_1 = \frac{1}{\beta_1}, SDRL_1 = \sqrt{\frac{1-\beta_1}{\beta_1^2}}, \tag{33}$$

where β_1 denotes the Type II error. In this case, ARL_1 is used to evaluate $SDRL_1$ via Equation 24. These metrics help determine how effectively a control chart detects process shifts, with lower values of ARL_1 and $SDRL_1$ indicating better performance in identifying alterations in the process means.

One further key parameter is the average extra quadratic loss (AEQL) [32], which measures the average cost or deviation resulting from out-of-control states. The AEQL measures the mean squared deviation from the target value during such periods and is given by:

$$AEQL = \frac{1}{\Delta}\sum_{\delta_i=\delta_{min}}^{\delta_{max}\sum ARL_{\delta_i}} \delta_i \times ARL \tag{34}$$

here, δ_i indicates process shift magnitude for the ith scenario, while Δ indicates the total range of change values from δ_{min} to δ_{max}. Our investigation sets Δ as 13, covering shift values from $\delta = 0.001$ to $\delta = 1$. To detect process changes, it is expected that greater effectiveness would be displayed by a control chart for which the AEQL is lower.

To further assess chart performance, the Performance Comparison Index (PCI) [33] is employed. This PCI provides a relative efficiency measure by taking a specific control chart and comparing its AEQL to the AEQL of the chart which performed best (the one for which the AEQL was lowest). The definition is as follows:

$$PCI = \frac{AEQL}{AEQL_{min}} \tag{35}$$

In general, if the value for PCI equals 1, this indicates the most efficient control chart, balancing the ability to detect out-of-control conditions promptly while minimizing false alarms.

Tables 3 and 4 present data from the EWMA and modified EWMA charts allowing comparisons of efficiency to be drawn under various parameter settings for the respective ARMA(2,2) and ARMA(3,3) models. The smoothing parameters $\lambda = 0.1$ and $\lambda = 0.2$ were applied to reflect differences in responsiveness to shifts. Additionally, various model coefficients were considered, while the in-control ARL_0 was fixed at 370.

Table 3. Comparison of the ARLs for the ARMA(2,2) model of the EWMA and modified EWMA through the explicit formula when $\mu = 2, k = 0.5$, ARL$_0$=370

Parameter	δ	$\lambda = 0.1$				$\lambda = 0.2$			
		EWMA		MEWMA		EWMA		MEWMA	
		ARL	SDRL	ARL	SDRL	ARL	SDRL	ARL	SDRL
	UCL	h=0.0007225		b =0.230249		h=0.029439		b =0.2428527	
	0.000	370.0226	369.5222	370.0441	369.5438	370.0519	369.5515	370.0660	369.5663
	0.001	365.6526	365.1523	310.3312	309.8308	360.4241	359.9237	289.4503	288.9498
	0.003	357.0919	356.5916	324.4370	233.9365	342.3979	341.8975	201.5167	201.0161
	0.005	348.7642	348.2638	188.2191	187.7185	325.8470	325.3466	154.4888	153.9880
	0.007	340.6622	340.1618	157.1197	156.6189	310.6011	310.1007	125.2107	124.7097
	0.01	328.9175	328.4171	125.7894	125.2884	289.8676	289.3672	97.4435	96.9422
$\phi_i = 0.3$	0.03	261.6690	261.1685	53.3421	52.8397	195.2588	194.7582	39.0820	38.5787
$\theta_i = 0.4$	0.05	209.9763	209.4757	33.4303	32.9265	142.0396	141.5387	24.3102	23.8049
	0.07	169.8805	169.3798	24.1502	23.6449	108.4570	107.9558	17.5904	17.0831
	0.10	125.4233	124.9223	16.8982	16.3905	76.8776	76.3760	12.4043	11.8938
	0.30	23.9836	23.4782	5.3916	4.8660	17.7704	17.2632	4.2439	3.7103
	0.50	7.5407	7.0229	3.2528	2.7070	7.5934	7.0758	2.7088	2.1515
	0.70	3.4653	2.9228	2.4233	1.8571	4.3417	3.8090	2.1022	1.5222
	1.00	1.8055	1.2060	1.8662	1.2715	2.5720	2.0108	1.6868	1.0764
	AEQL	0.7469		0.3428		0.7203		0.2931	
	PCI	2.5478		1.1694		2.4571		1.0000	
	UCL	h=0.0002652		b =0.0835854		h=0.0106801		b =0.2428527	
	0.000	370.0078	369.5075	370.0148	369.5144	370.0143	369.5140	370.0224	369.5221
	0.001	365.2566	364.7563	292.8953	292.3949	357.8369	357.3366	267.4804	266.9800
	0.003	355.9642	355.4638	206.4772	205.9766	335.4617	334.9614	171.9606	171.4599
	0.005	346.9438	346.4434	159.2421	158.7414	315.3918	314.8914	126.6145	126.1135
	0.007	338.1867	337.6863	129.4683	128.9673	297.2937	296.7932	100.1344	99.6331
	0.01	325.5257	325.0253	100.9678	100.4666	273.2617	272.7612	76.1602	75.6585
$\phi_i = -0.2$	0.03	253.8573	253.3568	40.2402	39.7371	171.4984	17.9976	29.0803	28.5760
$\theta_i = -0.6$	0.05	199.8645	199.3638	24.7169	24.2117	119.5030	119.0020	17.8324	17.3252
	0.07	158.7828	158.2820	17.6528	17.1455	88.5253	88.0239	12.8070	12.2969
	0.10	114.2425	113.7414	12.2170	11.7063	60.6979	60.1958	8.9738	8.4590
	0.30	19.1529	18.6462	3.8335	3.2958	12.6199	12.1096	3.0805	2.5316
	0.50	5.6617	5.1374	2.3615	1.7931	5.2239	4.6974	2.0271	1.4430
	0.70	2.6249	2.0653	1.8165	1.2179	3.0161	2.4660	1.6290	1.0123
	1.00	1.4863	0.8502	1.4676	0.8283	1.8850	1.2916	1.3687	0.7104
	AEQL	0.6158		0.2587		0.5251		0.2280	
	PCI	2.7013		1.1349		2.3034		1.0000	

Table 4. Comparison of the ARLs for the ARMA(3,3) model of the EWMA and modified EWMA under the explicit formula for $\mu = 2, k = 0.5$, ARL$_0$=370

| Parameter | δ | $\lambda = 0.1$ | | | | $\lambda = 0.2$ | | | |
| | | EWMA | | MEWMA | | EWMA | | MEWMA | |
		ARL	SDRL	ARL	SDRL	ARL	SDRL	ARL	SDRL
	UCL	h=0.0010797		b =0.3470962		h=0.0444		b =0.368956	
	0.000	370.0256	369.5253	370.0208	369.5205	370.0480	369.5476	370.0779	369.5775
	0.001	365.8086	365.3083	317.7350	317.2346	361.4285	360.9282	299.2019	298.7015
	0.003	357.5422	357.0419	247.5788	247.0783	345.1702	344.6698	216.2616	215.7610
	0.005	349.4939	348.9935	202.6703	202.1697	330.1026	329.6022	169.2630	168.7623
	0.007	341.6571	341.1567	171.4602	170.9595	316.1026	315.6022	139.0051	138.5042
	0.01	330.2847	329.7844	139.1738	138.6729	296.8750	296.3745	109.5672	109.0660
$\phi_i = 0.5$	0.03	264.8680	264.3675	61.0650	60.5629	206.2426	205.7420	45.2098	44.7070
$\theta_i = 0.7$	0.05	214.1760	213.6754	38.6965	38.1932	153.0130	152.5122	28.3548	27.8503
	0.07	174.5513	174.0506	28.1260	27.6215	118.4987	117.9976	20.6047	20.0985
	0.10	130.2182	129.7172	19.7936	19.2871	85.3136	84.8122	14.5835	14.0746
	0.30	26.2714	25.7665	6.3854	5.8641	20.7112	20.2050	5.0014	4.4736
	0.50	8.4951	7.9795	3.8328	3.2951	9.0024	8.4877	3.1607	2.6133
	0.70	3.9152	3.3784	2.8248	2.2704	5.1533	4.6263	2.4211	1.8549
	1.00	1.9867	1.4001	2.1358	1.5575	3.0069	2.4566	1.9056	1.3136
	AEQL	**0.8133**		**0.3979**		**0.8361**		**0.3368**	
	PCI	**2.4151**		**1.1814**		**2.4827**		**1.0000**	
	UCL	h=0.0004376		b =0.1385002		h=0.017701		b =0.145218	
	0.000	370.0052	369.5049	370.0281	369.5278	370.0024	369.5021	370.0199	369.5196
	0.001	365.4446	364.9443	301.4948	300.9943	359.1075	358.6071	278.1334	277.6330
	0.003	356.5177	356.0173	219.7885	219.2879	338.8985	338.3981	185.7199	185.2192
	0.005	347.8429	347.3426	172.7512	172.2504	320.5585	320.0581	139.3158	138.8149
	0.007	339.4123	338.9119	142.1811	141.6802	303.8441	303.3437	111.4112	110.9101
	0.01	327.2073	326.7070	112.2222	111.7211	281.3861	280.8856	85.6134	85.1119
$\phi_i = -0.8$	0.03	257.7234	257.2229	45.9930	45.4902	182.7698	182.2691	33.4080	32.9042
$\theta_i = -0.9$	0.05	204.8473	204.3467	28.5067	28.0022	129.9992	129.4982	20.6153	20.1091
	0.07	164.2269	163.7261	20.4648	19.9585	97.6957	97.1944	14.8543	14.3456
	0.10	119.6911	119.1900	14.2334	13.7243	68.0503	67.5484	10.4368	9.9242
	0.30	21.4214	20.9154	4.4942	3.9627	14.8814	14.3727	3.5702	3.0292
	0.50	6.5201	5.9993	2.7353	2.1786	6.2470	5.7252	2.3112	1.7408
	0.70	3.0008	2.5403	2.0686	1.4868	3.5812	3.0403	1.8245	1.2265
	1.00	1.6257	1.0085	1.6313	1.0148	2.1734	1.5970	1.4987	0.8645
	AEQL	**0.6758**		**0.2938**		**0.6095**		**0.2550**	
	PCI	**2.6502**		**1.1522**		**2.3900**		**1.0000**	

Table 3, which summarizes the results related to the ARMA(2,2) model, reveals that the modified EWMA chart generally yields smaller values in the case of ARL$_1$ and SDRL$_1$ than is the case for the standard EWMA chart. The only

exception occurred when $\delta = 1$ and all coefficient parameters were positive. In all other scenarios, especially when $\lambda = 0.2$, the modified EWMA chart consistently outperforms the standard EWMA chart. This suggests that increasing the smoothing parameter improves the chart's responsiveness, allowing quicker identification of mean shifts, especially in more volatile or positively autocorrelated processes.

To further verify the performance, both AEQL and PCI values were calculated taking into consideration the ARL values via Equations 32 and 33. Table 3 shows outcomes which confirm that the smallest AEQL and a PCI of 1 are achieved by a modified EWMA chart when $\lambda = 0.2$, indicating optimal efficiency in detecting out-of-control conditions. These secondary indicators reinforce the value of using the modified chart for early and accurate detection in complex autocorrelated environments.

Table 4, which presents the results for the ARMA(3,3) model, shows similar trends. The modified EWMA control chart again outperforms the standard EWMA chart in most cases, except for $\delta = 1$, where the performance was comparable or slightly less favorable. Nonetheless, for $\lambda = 0.2$, the modified EWMA consistently provides lower ARL$_1$ and SDRL$_1$ values in all the tested scenarios. This consistency across different model structures (ARMA(2,2) and ARMA(3,3)) highlights the modified EWMA's robustness across various time series configurations.

As with the previous model, Table 4 shows AEQL and PCI values which confirm the superior performance of the modified EWMA chart at $\lambda = 0.2$. This version of the chart yielded the lowest AEQL and a PCI of 1, reinforcing its suitability for detecting process shifts efficiently. These findings highlight the chart's practical advantage in applications where rapid anomaly detection is crucial, such as environmental monitoring.

Overall, the results from Tables 3 and 4 suggest that setting $\lambda = 0.2$ in the modified EWMA chart offers optimal performance in identifying changes in the ARMA(2,2) and ARMA(3,3) processes and can be confidently applied in real-world process monitoring applications. This conclusion not only supports the findings of previous studies but also expands the applicability of the modified chart to more generalized and complex ARMA(p,q) structures.

4-2- Implementation with Authentic Data

In this study, daily average PM2.5 concentrations from three provinces in Thailand—Nakhon Phanom, Nan, and Nonthaburi—were analyzed via a dataset comprising 366 observations acquired during January 1 to December 31, 2024. Each dataset was modeled via ARMA(p,q) processes, with model selection based on t statistics for the Box–Jenkins methodology implemented using SPSS. Residuals (white noise) from the fitted models subsequently underwent testing for an exponential distribution via the one-sample Kolmogorov–Smirnov test.

Specifically, the average daily PM2.5 levels (measured in µg/m³) are as follows:

Nakhon Phanom, were best modeled by an ARMA(2,1) process, represented as:

$$X_t = 45.565 - 0.106X_{t-1} + 0.875X_{t-2} - 1.000\theta_{t-1} + \varepsilon_t; \varepsilon_t \sim \text{Exp}(\alpha_0 = 12.2385). \tag{36}$$

Nan were modeled as an ARMA(2,2) process, as shown below:

$$X_t = 35.521 + 1.685X_{t-1} - 0.689X_{t-2} + 0.499\theta_{t-1} + 0.356\theta_{t-2} + \varepsilon_t; \varepsilon_t \sim \text{Exp}(\alpha_0 = 4.4426). \tag{37}$$

Nonthaburi were fitted via an ARMA(3,3) model, shown as:

$$X_t = 37.168 + 0.484X_{t-1} + 0.980X_{t-2} - 0.470X_{t-3} - 0.407\theta_{t-1} + 0.883\theta_{t-2} + 0.308\theta_{t-3} + \varepsilon_t;$$
$$\varepsilon_t \sim \text{Exp}(\alpha_0 = 6.4214). \tag{38}$$

To evaluate the proposed modified EWMA control chart performance, these real-world autocorrelated datasets were evaluated under various shift sizes (δ =0.001, 0.003, 0.005, 0.01, 0.03, 0.05, 0.1, 0.3, 0.5, and 1.0), whereby the in-control ARL$_0$ was set to 370. Table 5 shows the comparison findings of the ARL and SDRL for both the standard EWMA and the modified EWMA control charts under all of the ARMA(p, q) settings.

Table 5. Efficiency comparison for authentic data fitted to an ARMA(p,q) model of EWMA and modified EWMA using an explicit formula at ARL$_0$=370

Model	δ	$\lambda = 0.1$				$\lambda = 0.2$			
		EWMA		MEWMA		EWMA		MEWMA	
		ARL	SDRL	ARL	SDRL	ARL	SDRL	ARL	SDRL
	UCL	h=0.02547203		b =0.1640327		h=0.05109264		b =0.1897428	
	0.000	370.0064	369.5061	370.0783	369.5780	370.0111	369.5108	370.0228	369.5224
	0.001	197.6544	197.1538	143.5023	143.0015	160.5157	160.0149	140.9085	140.4076
	0.003	102.3437	101.8424	64.7953	64.2934	75.4790	74.9774	63.2462	62.7442
	0.005	69.0606	68.5587	42.0028	41.4998	49.4565	48.9540	40.9369	40.4338
	0.01	38.1122	37.6089	22.5440	22.0383	26.7102	26.2054	21.9541	21.4483
ARMA(2,1)	0.03	13.7081	13.1986	8.2439	7.7278	9.6752	9.1616	8.0408	7.5242
	0.05	8.4130	7.8972	5.2486	4.7222	6.0742	5.5517	5.1303	4.6033
	0.10	4.3821	3.8498	2.9838	2.4329	3.3476	2.8034	2.9302	2.3782
	0.30	1.7979	1.1978	1.5112	0.8790	1.5850	0.9629	1.4990	0.8648
	0.50	1.3627	0.7030	1.2485	0.5571	1.2772	0.5950	1.2431	0.5497
	1.00	1.1114	0.3519	1.0853	0.3043	1.0911	0.3153	1.0837	0.3012
	AEQL	0.1543		0.1443		0.1468		0.0511	
	PCI	3.0188		2.8234		2.8720		1.0000	
	UCL	h=0.0001539607		b =0.001132956		h=0.0003121721		b =0.0012872346	
	0.000	370.0032	369.5029	370.0217	369.5213	370.0085	369.5082	370.0096	369.5092
	0.001	255.6730	255.1725	112.0007	111.4996	157.5025	157.0017	105.6652	105.1640
	0.003	157.2420	156.7412	46.9767	46.4740	73.2171	72.7154	43.7431	43.2402
	0.005	112.9983	112.4972	29.8320	29.3277	47.6492	47.1466	27.7079	27.2033
	0.01	65.5418	65.0399	15.7337	15.2255	25.3917	24.8867	14.6110	14.1022
ARMA(2,2)	0.03	22.9948	22.4892	5.6866	5.1624	8.8083	8.2932	5.3256	4.7996
	0.05	13.1953	12.6854	3.6260	3.0858	5.3389	4.8130	3.4256	2.8826
	0.10	5.8065	5.2829	2.0999	1.5197	2.7702	2.2145	2.0184	1.4338
	0.30	1.6504	1.0361	1.1901	0.4756	1.2780	0.5960	1.1775	0.4571
	0.50	1.1869	0.4710	1.0659	0.2650	1.0895	0.3123	1.0619	0.2564
	1.00	1.0256	0.1621	1.0123	0.1116	1.0148	0.1225	1.0117	0.1086
	AEQL	0.1449		0.1294		0.1323		0.1290	
	PCI	1.1228		1.0032		1.0256		1.0000	
	UCL	h=0.00216129		b =0.01487649		h=0.004348884		b =0.0170434	
	0.000	370.0342	369.5338	370.0304	369.5300	370.0108	369.5105	370.0099	369.5096
	0.001	228.9974	228.4969	126.9621	126.4611	158.9734	158.4726	122.1987	121.6977
	0.003	129.5869	129.0860	55.1177	54.6154	74.3316	73.8300	52.5005	51.9981
	0.005	90.1334	89.6320	35.3332	34.8296	48.5473	48.0447	33.5767	33.0729
	0.01	50.8683	50.3659	18.7854	18.2785	26.0563	25.5514	17.8366	17.3294
ARMA(3,3)	0.03	18.0183	17.5112	6.8262	6.3064	9.2531	8.7388	6.5102	5.9894
	0.05	10.6918	10.1795	4.3477	3.8151	5.7162	5.1922	4.1676	3.6334
	0.10	5.1313	4.6042	2.4900	1.9261	3.0620	2.5127	2.4121	1.8456
	0.30	1.7570	1.1532	1.3231	0.6539	1.4190	0.7711	1.3081	0.6348
	0.50	1.2800	0.5987	1.1360	0.3930	1.1677	0.4426	1.1302	0.3836
	1.00	1.0598	0.2518	1.0359	0.1930	1.0408	0.2060	1.0346	0.1893
	AEQL	0.1492		0.1349		0.1380		0.1344	
	PCI	1.1099		1.0039		1.0269		1.0000	

According to our findings, the modified EWMA chart consistently produces lower ARL_1 and $SDRL_1$ values across all shift sizes and all three models, indicating faster and more accurate identification of scenarios which are out of control. By contrast, the original EWMA chart often shows substantially higher ARL_1 and $SDRL_1$ values, especially under larger shifts, which could delay detection. This further emphasizes that the modified chart offers greater efficacy in more rapidly identifying process shifts, reducing time lags between the actual occurrence of a shift and its identification, which is essential for timely corrective actions in air quality monitoring.

Moreover, additional performance measures—AEQL and PCI—were calculated to further validate how effective each control chart was. The modified EWMA chart, particularly using higher $\lambda = 0.2$ values, consistently yielded the lowest AEQL values while the PCI was 1 is each case, demonstrating the better level of performance. These real-world results align closely with the simulation findings and highlight the modified EWMA control chart's enhanced sensitivity and robustness when monitoring auto-correlated PM2.5 data modeled by the ARMA(2,1), (2,2), and (3,3) procedures, which is further demonstrated by the comparative results presented in Table 5. The combination of low AEQL and perfect PCI reveals that our modified EWMA chart is capable of earlier identification in addition to minimizing the costs associated with delayed detection, reinforcing its practical value for high-stakes applications such as environmental health surveillance.

On the basis of the findings discussed earlier, the control chart performance, particularly their sensitivity in detecting process mean shifts, has been validated via a dataset of 366 observations under the ARMA(p,q) model framework. This research made use of control charts which were designed to feature a UCL along with a fixed LCL of zero ($a = 0$). Accordingly, under these terms, the control chart was one sided, deviating from the conventional symmetric structure typically used in general process monitoring. This design choice reflects a domain-specific adaptation, ensuring that the chart responds only to undesirable increases in PM2.5 levels, which are directly linked to health hazards.

This one-sided approach is purposefully employed to align with the characteristics of PM2.5 concentration data. Unlike general process parameters, which may fluctuate both above and below the target value, the PM2.5 concentration should ideally remain as low as possible since elevated levels are directly associated with poor health, such as respiratory and cardiovascular problems. In contrast, lower concentrations are favorable and do not require intervention. Hence, the asymmetric configuration enhances the chart's practical utility, as it focuses exclusively on upward shifts in the data that may indicate deteriorating air quality. This reflects the real-world requirements of environmental monitoring systems, where early detection of increased pollution levels is of primary concern. Thus, the tailored chart design ensures the method's applicability in real-life monitoring scenarios, prioritizing human health outcomes over purely statistical symmetry.

To compare our proposed chart to the traditional EWMA chart in the context of effectiveness, the shift identification capabilities were assessed via real-world PM2.5 data modeled via various ARMA processes. The data were collected from three representative provinces in Thailand—each selected from a different geographical region, namely, the Northeast, North, and Central regions—to ensure regional diversity in the analysis. These provinces were chosen because of their historical records of elevated PM2.5 amounts, especially around January – May when air pollution problems tend to intensify. An exponential smoothing parameter of $\lambda = 0.2$ was used for both charts to improve responsiveness to subtle shifts. The control charts were then used to investigate authentic data, with comparative results illustrated in Figures 2 to 4.
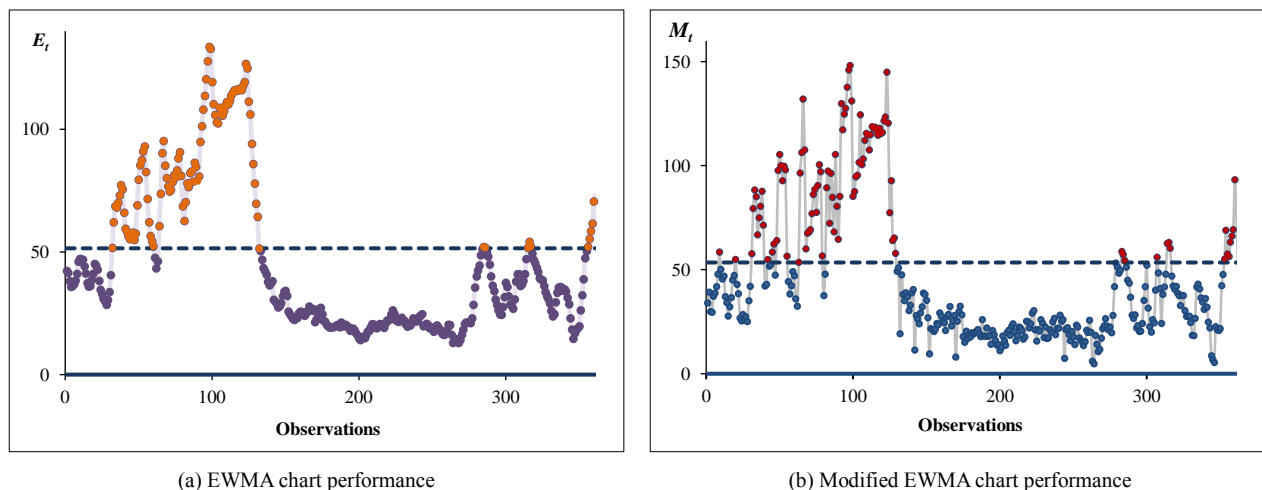

(a) EWMA chart performance   (b) Modified EWMA chart performance

Figure 2. Detection performance of the EWMA and modified EWMA charts under the ARMA(2, 1) procedure

(a) EWMA chart performance

(b) Modified EWMA chart performance
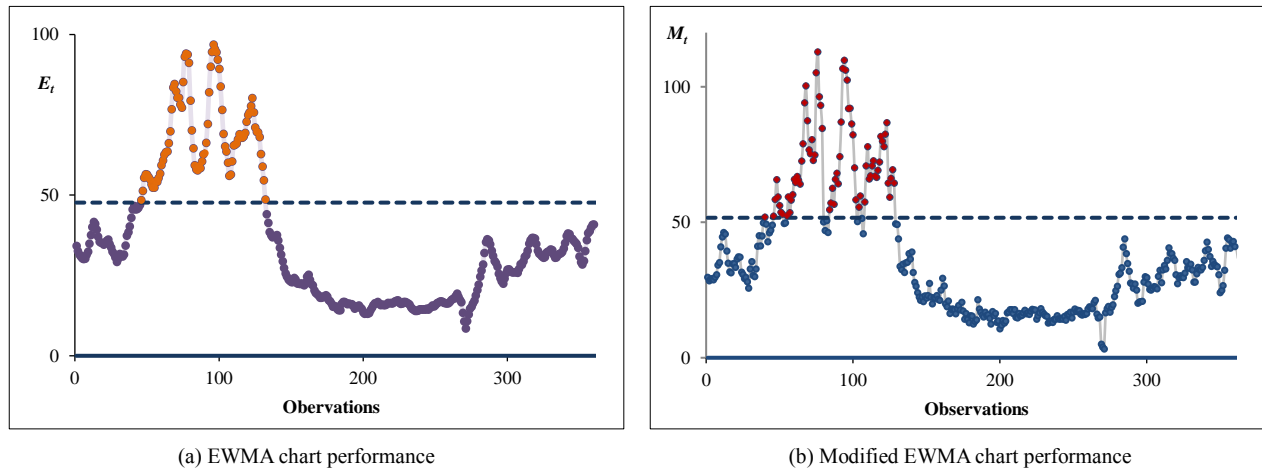
Figure 3. Detection performance of the EWMA and modified EWMA charts for the ARMA(2,2) procedure

(a) EWMA chart performance

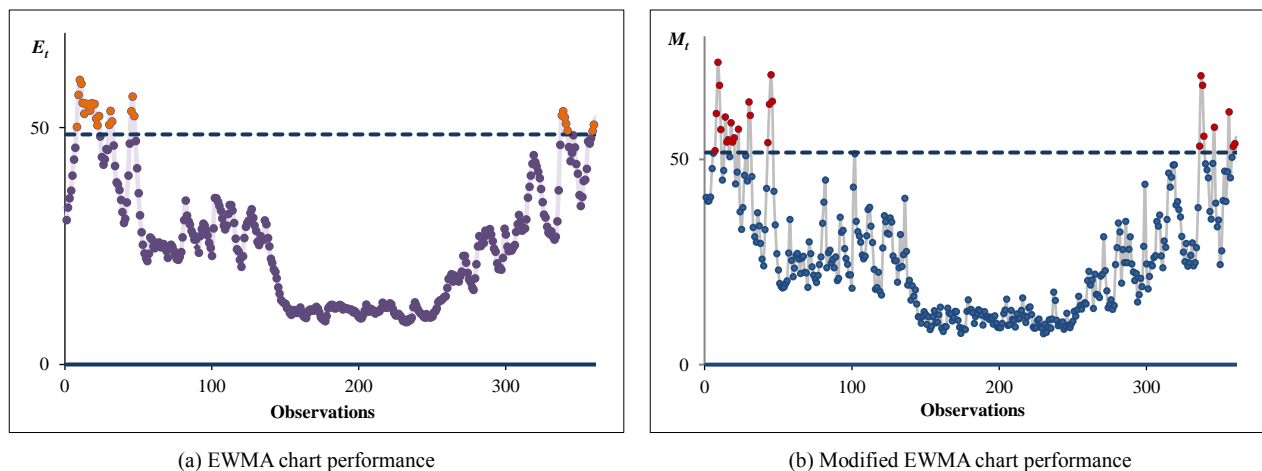(b) Modified EWMA chart performance

Figure 4. Detection performance of the EWMA and modified EWMA charts under the ARMA(3,3) procedure

Figure 2 displays control chart outcomes for the PM2.5 data modeled via an ARMA(2, 1) process, which were fitted with average daily concentration data from Nakhon Phanom Province. The standard EWMA chart was able to identify a process mean shift at the 32nd sample point, but the modified EWMA chart successfully detected such changes earlier—at the 9th sample point. This considerable improvement in early detection demonstrates the enhanced sensitivity of the modified chart in cases where it is used with autocorrelated environmental data. The modified EWMA structure, which incorporates additional smoothing features, facilitates faster recognition of deviations from normal conditions, which is particularly critical in time-sensitive air quality monitoring. This result demonstrates that the modified EWMA chart offers greater efficacy in identifying early warning signs of pollution level increases, allowing for more proactive responses to environmental risks. The improvement in detection time could translate into earlier mitigation efforts, such as public health alerts or temporary emission controls.

In Figure 3, the PM2.5 data from Nan Province were modeled via an ARMA(2,2) process. The modified EWMA chart again outperforms a traditional EWMA chart by detecting a change at the 40th sample point, whereas the traditional chart does not signal a shift until the 46th point. Although the detection times are relatively close, the modified EWMA chart shows a consistent advantage in terms of responsiveness. This reinforces its suitability for real-time surveillance, where even small delays in detection could lead to insufficient reaction time to harmful pollution episodes.

Furthermore, the narrow gap in detection points emphasizes the strength of the modified chart in maintaining both sensitivity and stability under complex autocorrelated structures. This finding suggests that even subtle process mean changes can be captured with greater reliability, supporting the chart's robustness across different time series models.

Figure 4 presents the detection comparison for the PM2.5 data from Nonthaburi Province, which were modeled via an ARMA(3,3) process. Interestingly, the traditional and modified EWMA control charts both demonstrated the ability to reveal a process shift at the 8th sample point. This finding indicates that, in certain cases where the shift is pronounced and the model structure is more complex, both charts may perform similarly. In every one of the situations evaluated, however, the modified EWMA chart proved equal to or better than the traditional version in terms of early detection and stability.

This consistency highlights the reliability of the proposed method, especially in practical applications where varying noise patterns and data characteristics can affect control performance. Even when traditional charts succeed, the modified chart ensures comparable or better results, validating its applicability to real-world environmental monitoring challenges.

5- Discussion

Our research clearly demonstrates the importance of enhancing control chart methods to monitor autocorrelated processes, particularly those modeled via ARMA(p,q) structures with exponential white noise. Such models better reflect the nonnormal, time-dependent nature of real-world data such as PM2.5 concentrations. A key contribution of this research is the ARL explicit formula, which provides exact values that are consistent with the well-established NIE while significantly reducing the computation time required for ARL estimation. This computational efficiency is especially valuable during the design and calibration phases of control chart development. This reduced computation time refers specifically to the determination of ARL values, and could be considered critical in implementing control charts in terms of the design and tuning. The ability to perform these calculations quickly enables more efficient deployment and real-time adjustment of control charts, particularly in high-frequency or real-time monitoring scenarios, such as those encountered in environmental or industrial applications. Furthermore, the proposed chart's design—particularly its one-sided control limits—reflects a practical adaptation for scenarios where increases in the monitored variable, such as pollution levels, are of primary concern.

Another important factor contributing to modified EWMA chart effectiveness is the smoothing parameter (λ) choice. This study adopted a λ value of 0.20 on the basis of evidence that higher values enhance the capacity of a chart to identify minor changes in the process mean. Prior research supports this approach: Paichit & Peerajit [34] reported that a modified EWMA chart with λ =0.10 outperformed its standard counterpart, and Phanthuna & Areepong [25] further demonstrated that λ =0.20 yielded the most efficient detection compared with smaller values. These results concur with those reported by Supharakonsakun et al. [35] and reinforce the configuration of the current study. Together, these enhancements—the explicit ARL formulation and optimized smoothing parameter—solidify the modified EWMA chart as a robust and sensitive tool capable of observing and detecting subtle process changes in complex, real-world data environments.

However, one limitation of the current study is that the analysis was conducted under the assumption that the data follow an ARMA(p,q) model without seasonal components. In real-world scenarios, especially with environmental data such as PM2.5, seasonal effects are common and may require more complex models such as Seasonal ARMA (SARMA) or other time series structures. Future research should explore the performance and adaptability of the proposed control chart under such seasonal or misspecified models to extend its practical applicability. Although the current study focuses on univariate time series data, this approach can be extended to monitor various types of individual environmental indicators, such as PM2.5, PM10, or NO_2. It can also be adapted for public health surveillance (e.g., tracking disease incidence or hospital admissions), industrial process control, and other domains where timely detection of subtle shifts in autocorrelated data is crucial. This broadens the chart's potential impact, offering decision-makers a robust tool for early intervention and prevention in both environmental and healthcare contexts. However, future research could explore the extension of this method to multivariate time series, where multiple indicators are monitored simultaneously. This presents important challenges, such as handling intervariable autocorrelation and developing a multivariate control chart structure that maintains sensitivity and robustness across variables. These complexities highlight a promising direction for further study.

6- Conclusion

This study introduces a modified EWMA control chart supported by a novel, explicit formula used to calculate the ARL in ARMA(p,q) processes with exponential white noise. Our proposed method not only matches the Numerical Integral Equation (NIE) approach in accuracy but also substantially outperforms it in computational efficiency. Comparative analyses involving both synthetic ARMA datasets and real-world PM2.5 observations from three Thai provinces demonstrate the superior performance of the modified chart—particularly its sensitivity to small process shifts and lower false alarm rates. With consistent PCI scores of 1 and reduced AEQL, the modified chart proves to be an effective monitoring tool. Moreover, the application to environmental data shows that the chart adapts well to complex, autocorrelated time series, making it highly relevant for air quality surveillance. The use of asymmetric, one-sided control limits enhances the chart's practicality in contexts where only increases in process values—such as pollution levels—are of concern. Overall, the modified EWMA chart, coupled with its efficient ARL computation method, presents valuable advancements in statistical process control, offering both theoretical rigor and real-world applicability in environmental and industrial monitoring.

7- Declarations

7-1- Author Contributions

Conceptualization, Y.S. and Y.A.; methodology, Y.S.; software, Y.S. and Y.A.; validation, Y.S. and Y.A.; formal analysis, Y.S.; investigation, Y.S.; resources, Y.S.; data curation, Y.S.; writing—original draft preparation, Y.S.; writing—review and editing, Y.S. and Y.A.; visualization, Y.S.; supervision, Y.A.; project administration, Y.S.; funding acquisition, Y.S. All authors have read and agreed to the published version of the manuscript.

7-2- Data Availability Statement

The dataset utilized during the course of this research consists of historical PM2.5 concentration levels recorded across various provinces in Thailand. These real-world data for air quality data was acquired from the official website of the Pollution Control Department (PCD), Ministry of Natural Resources and Environment, Air4Thai. The dataset is publicly accessible through the following link: *http://air4thai.pcd.go.th/webV3/#/History*.

7-3- Funding

7-4- Institutional Review Board Statement

Not applicable.

7-5- Informed Consent Statement

Not applicable.

7-6- Conflicts of Interest

The authors declare that there is no conflict of interest regarding the publication of this manuscript. In addition, the ethical issues, including plagiarism, informed consent, misconduct, data fabrication and/or falsification, double publication and/or submission, and redundancies have been completely observed by the authors.

8- References

[1] Ni, H., Tian, J., Wang, X., Wang, Q., Han, Y., Cao, J., Long, X., Chen, L. W. A., Chow, J. C., Watson, J. G., Huang, R. J., & Dusek, U. (2017). PM2.5 emissions and source profiles from open burning of crop residues. Atmospheric Environment, 169, 229–237. doi:10.1016/j.atmosenv.2017.08.063.

[2] World Health Organization (WHO). (2021). WHO global air quality guidelines: Particulate matter (PM2.5 and PM10), ozone, nitrogen dioxide, sulfur dioxide and carbon monoxide. World Health Organization (WHO), Geneva, Switzerland.

[3] Suriyawong, P., Chuetor, S., Samae, H., Piriyakarnsakul, S., Amin, M., Furuuchi, M., Hata, M., Inerb, M., & Phairuang, W. (2023). Airborne particulate matter from biomass burning in Thailand: Recent issues, challenges, and options. Heliyon, 9(3), 14261. doi:10.1016/j.heliyon.2023.e14261.

[4] Guo, J., Chai, G., Song, X., Hui, X., Li, Z., Feng, X., & Yang, K. (2023). Long-term exposure to particulate matter on cardiovascular and respiratory diseases in low- and middle-income countries: A systematic review and meta-analysis. Frontiers in Public Health, 11, 1134341. doi:10.3389/fpubh.2023.1134341.

[5] Pun, V. C., Kazemiparkouhi, F., Manjourides, J., & Suh, H. H. (2017). Long-Term PM2.5 Exposure and Respiratory, Cancer, and Cardiovascular Mortality in Older US Adults. American Journal of Epidemiology, 186(8), 961–969. doi:10.1093/aje/kwx166.

[6] World Bank. (2022). Thailand economic monitor: The environmental impact of air pollution. The World Bank Group, Washington, United States.

[7] Emprasertsuk, W., Tansawet, A., Wabina, R. S. R., & Suppasilp, C. (2025). Association between Wildfire area and PM2.5 levels on the Prevalence of Mental disorders in Thailand. Environmental Challenges, 20, 101184. doi:10.1016/j.envc.2025.101184.

[8] Kliengchuay, W., Wen, B., Aye, T. S., Aung, H. W., Suwanmanee, S., Tawatsupa, B., Laor, P., Kongpran, J., Wongsantichon, J., Xu, R., Li, S., Hashizume, M., Guo, Y., & Tantrakarnapa, K. (2025). Effect modification of fine particulate matter (PM2.5) related hospital admissions by temperature in Thailand: A nationwide time-series study. Environmental Research, 277, 121467. doi:10.1016/j.envres.2025.121467.

[9] Wongwatcharapaiboon, J. (2020). Review Article: Toward future particulate matter situations in Thailand from supporting policy, network and economy. Future Cities and Environment, 6(1),79. doi:10.5334/fce.79.

[10] W.H.O. (2021). Health effects of particulate matter: Policy implications for countries in eastern Europe, Caucasus and central Asia. World Health Organization (W.H.O.), Geneva, Switzerland.

[11] Soontornpipit, P., Lekawat, L., Tritham, C., Tritham, C., Pongpaibool, P., Prasertsuk, N., & Jirakitpuwapat, W. (2024). PM2.5 Prediction & Air Quality Classification UsinMachine Learning. Thai Journal of Mathematics, 22(2), 441-452.

[12] Montgomery, D. C. (2020). Introduction to statistical quality control. John Wiley & Sons, Hoboken, United States.

[13] da Silva, G. J., & Borges, A. C. (2025). Statistical Process Control in the Environmental Monitoring of Water Quality and Wastewaters: A Review. Water (Switzerland), 17(9), 1281. doi:10.3390/w17091281.

[14] Arciszewski, T. J. (2023). A Review of Control Charts and Exploring Their Utility for Regional Environmental Monitoring Programs. Environments, 10(5), 78. doi:10.3390/environments10050078.

[15] Srisang, W., Jaroensutasinee, K., Jaroensutasinee, M., Khongthong, C., Piamonte, J. R. P., & Sparrow, E. B. (2024). PM2.5 IoT Sensor Calibration and Implementation Issues Including Machine Learning. Emerging Science Journal, 8(6), 2267–2277. doi:10.28991/ESJ-2024-08-06-08.

[16] Shewhart, W. A. (2022). Economic control of quality of manufactured product. Barakaldo Books, London, United Kingdom.

[17] Page, E. S. (1954). Continuous Inspection Schemes. Biometrika, 41(1/2), 100. doi:10.2307/2333009.

[18] Roberts, S. W. (1959). Control Chart Tests Based on Geometric Moving Averages. Technometrics, 1(3), 239–250. doi:10.1080/00401706.1959.10489860.

[19] Khan, Z., Saghir, A., Katona, A., & Kosztyán, Z. T. (2025). EWMA control chart framework for efficient Maxwell quality characteristic monitoring: An application to the aerospace industry. Computers & Industrial Engineering, 200, 110753. doi:10.1016/j.cie.2024.110753.

[20] Kazmi, M. W., & Noor-ul-Amin, M. (2025). Integrating machine learning based EWMA control charts for multivariate process monitoring. Computers & Industrial Engineering, 204, 111131. doi:10.1016/j.cie.2025.111131.

[21] Patel, A. K., & Divecha, J. (2011). Modified exponentially weighted moving average (EWMA) control chart for an analytical process data. Journal of Chemical Engineering and Materials Science, 2(1), 12-20.

[22] Khan, N., Aslam, M., & Jun, C. (2016). Design of a Control Chart Using a Modified EWMA Statistic. Quality and Reliability Engineering International, 33(5), 1095–1104. doi:10.1002/qre.2102.

[23] Rasheed, Z., Zhang, H., Khan, M., & Anwar, S. M. (2025). Modified exponentially weighted moving average control chart for monitoring process dispersion. Communications in Statistics-Simulation and Computation, 54(9), 3545-3572. doi:10.1080/03610918.2024.2358137.

[24] Supharakonsakun, Y., & Areepong, Y. (2023). ARL Evaluation of a DEWMA Control Chart for Autocorrelated Data: A Case Study on Prices of Major Industrial Commodities. Emerging Science Journal, 7(5), 1771–1786. doi:10.28991/ESJ-2023-07-05-020.

[25] Phanthuna, P., & Areepong, Y. (2022). Detection Sensitivity of a Modified EWMA Control Chart with a Time Series Model with Fractionality and Integration. Emerging Science Journal, 6(5), 1134–1152. doi:10.28991/ESJ-2022-06-05-015.

[26] Imtiaz, A., Khan, N., Saleem, M., & Aslam, M. (2025). Development and application of a modified EWMA control chart for early detection of process shifts in skewed distributions. Journal of the Chinese Institute of Engineers, 48(5), 680–690. doi:10.1080/02533839.2025.2479121.

[27] Niaz, A., Khan, M., & Ijaz, M. (2025). One-Sided Modified EWMA Control Charts for Monitoring Time Between Events. Quality and Reliability Engineering International, 41(4), 1293–1318. doi:10.1002/qre.3718.

[28] Khamrod, S., Areepong, Y., Sukparungsee, S., & Sunthornwat, R. (2024). One-Sided and Two-Sided New Modified EWMA control chart for Detecting Increases in Process Mean. WSEAS Transactions on Systems and Control, 19, 473–488. doi:10.37394/23203.2024.19.50.

[29] Karoon, K., Areepong, Y., & Sukparungsee, S. (2023). Modification of ARL for detecting changes on the double EWMA chart in time series data with the autoregressive model. Connection Science, 35(1), 2219040. doi:10.1080/09540091.2023.2219040.

[30] Serrin, J. (1971). Gradient Estimates for Solutions of Nonlinear Elliptic and Parabolic Equations. Contributions to Nonlinear Functional Analysis, 565–601, Academic Press, Cambridge, United States. doi:10.1016/b978-0-12-775850-3.50017-0.

[31] Phanyaem, S. (2021). The integral equation approach for solving the average run length of EWMA procedure for autocorrelated process. Thailand Statistician, 19(3), 627–641.

[32] Fonseca, A., Ferreira, P. H., Do Nascimento, D. C., Fiaccone, R., Ulloa-Correa, C., García-Piña, A., & Louzada, F. (2021). Water particles monitoring in the Atacama desert: SPC approach based on proportional data. Axioms, 10(3), 154. doi:10.3390/axioms10030154.

[33] Alevizakos, V., Chatterjee, K., & Koukouvinos, C. (2022). The triple exponentially weighted moving average control chart for monitoring Poisson processes. Quality and Reliability Engineering International, 38(1), 532–549. doi:10.1002/qre.2999.

[34] Paichit, P., & Peerajit, W. (2022). The average run length for continuous distribution process mean shift detection on a modified EWMA control chart. Asia-Pacific Journal of Science and Technology, 27(6), 1-13..

[35] Supharakonsakun, Y., Areepong, Y., & Sukparungsee, S. (2020). Monitoring the Process Mean of a Modified EWMA Chart for ARMA(1,1) Process and Its Application. Suranaree Journal of Science and Technology, 27(4), 1–11.